Proceedings of the 15th International Heat Transfer Conference, IHTC-15
August 10-15, 2014, Kyoto, Japan

IHTC15-8857

MEASUREMENTS OF HEAT TRANSFER COEFFICIENTS TO CYLINDERS IN SHALLOW BUBBLE COLUMNS

Emily W. Tow[1,*] & John H. Lienhard V[1]

[1]Rohsenow Kendall Heat Transfer Laboratory, Massachusetts Institute of Technology
Cambridge, MA 02139, USA

ABSTRACT

High heat transfer coefficients and large interfacial areas make bubble columns ideal for dehumidification. However, the effect of geometry on the heat transfer coefficients outside cooling coils in shallow bubble columns, such as those used in multi-stage bubble column dehumidifiers, is poorly understood. The generally-overlooked entry and coalescing regions become important in shallow bubble columns, and there is disagreement on the effects of the coil and column diameters. In this paper, a method is presented for measuring the heat transfer coefficient between coil and liquid in a shallow bubble column. Horizontal cylindrical probes are used to measure the heat transfer coefficient over a range of gas velocities. The liquid depth and the diameter, height, and horizontal position of the cylinder are also varied. Existing correlations for tall columns tend to underpredict the heat transfer coefficient and do not account for all effects of geometry. The highest heat transfer coefficients (above 8000 W/m^2-K) are recorded on cylinders placed 4 cm high. No significant effect of cylinder diameter is observed. Based on the results, recommendations are made regarding bubble column dehumidifier design.

KEY WORDS: Two-phase/multiphase flow, turbulent transport, dehumidification, bubble column

1. INTRODUCTION

Shallow bubble columns are used as compact dehumidifiers in humidification-dehumidification (HDH) desalination systems [15, 21–23], but their unique geometry limits the applicability of existing correlations for heat transfer coefficients in tall columns. The effect of geometry on the heat transfer coefficient outside coils in shallow bubble columns, such as those used in multi-stage bubble column dehumidifiers, is poorly understood. Most of the literature on heat transfer in bubble columns focuses on the heat transfer coefficient at the column wall, although some studies address the heat transfer coefficient on internal heat exchange elements such as cylinders and helical coils. The studies involving internals, however, diagree on the effects of the column and heat exchange element diameters. The effects of additional geometric parameters relevant to shallow columns have not been studied.

Shallow bubble columns, which are desirable in HDH desalination because their low gas-side pressure drop reduces blowing power, have different fluid flow and heat transfer characteristics than tall columns. Because most bubble column reactors are orders of magnitude taller than those used for dehumidification [9, 15], the reactor modeling and design literature generally focuses on the developed flow region in the middle of the column and neglects to address the entry region near the bottom and the coalescing region near the free surface. In contrast, a shallow bubble column may have no developed (i.e., height-independent) flow. Heat transfer

*Corresponding Emily W. Tow: emilytow@mit.edu

coefficients on internal heat exchange elements (internals) in sieve-tray columns, which are similar in height to shallow bubble columns, have not been studied because sieve trays tend to be used without such elements.

Heat transfer in shallow bubble columns with internals differs from that in tall bubble columns due to the additional geometric parameters and the effect of the free surface on fluid dynamics. Bubble-on-coil impact, which depends on the horizontal position of the cylinder with respect to the sparger orifices, was proposed by Narayan et al. [15] as a geometric parameter of interest in shallow bubble columns with internals. The effects of coil diameter have been investigated by several authors, although there is disagreement among them [7, 10, 17]. The height of the cylinder is shown herein to affect heat transfer. In the present work, the effects and relative importance of these many parameters are investigated with the aim of guiding bubble column dehumidifier design.

1.1 Tall-Column Heat Transfer Coefficient Correlations

Perhaps the most widely used correlation for heat transfer from the gas-liquid mixture in a tall bubble column to a large surface such as the column wall is that of Deckwer [3], which is based on the idea that the bubbles' flow work is dissipated by small, energy-dissipating eddies which interact periodically with the heat transfer surface. The interactions are modeled as conduction through a semi-infinite slab with a characteristic time equal to the ratio of a characteristic eddy length and characteristic velocity. The application of an empirical constant leads to Deckwer's correlation [3], Equation 1, where the velocity in the dimensionless groups is the gas superficial velocity, u_g:

$$\mathrm{St} = 0.1(\mathrm{ReFrPr}^2)^{-1/4} \tag{1}$$

Hikita et al. compare a number of correlations and show that there is significant disagreement between them [5]. Most are semi-theoretical correlations that depend on the assumed mode of heat transfer. Many correlations echo Deckwer's [3], assuming thermal interaction with eddies produced by the dissipation of bubbles' flow work. Others consider fluid elements with a different length scale, such as the bubble diameter or distance between bubbles. Other disparities may be due to differences in measurement methods and, particularly in the case of correlations for internals, geometry.

Given that several reviews of bubble column heat transfer coefficient correlations already exist [6–9, 18, 19], the goal of this section is not to provide a thorough review of the subject. Rather, a small selection of correlations with a focus on those that apply to internals are presented to provide a background against which to view the experimental results. Table 1 gives a variety of correlations from the last five decades, four of which have one or more geometric parameters. The included geometric parameters, the relationship between heat transfer coefficient and superficial velocity, and the magnitude of the predicted heat transfer coefficient (as shown in [5]) all vary widely.

Table 1 Selected heat transfer coefficient correlations

Authors	Year	Application	Correlation
Konsetov [10][1]	1966	Internals	$\frac{\overline{h}\nu^2}{kg} = 0.18\left(\epsilon \mathrm{Pr}\frac{D_C}{D_p}\right)^{1/3}\left(\frac{\mu}{\mu_p}\right)^{0.14}$
Deckwer [3]	1980	Wall	$\mathrm{St} = 0.1(\mathrm{Re\ Fr\ Pr}^2)^{-1/4}$
Korte [8, 11]	1987	Tube bundle	$\mathrm{St} = 0.139(\mathrm{Re\ Fr\ Pr}^{2.26})^{-0.28}A_f^{-0.2}\left(\frac{D_C}{D_p}\right)^{0.14}\left(\frac{\mu}{\mu_p}\right)^{0.3}$
Saxena and Patel [17]	1991	Internals	$\overline{h} = 14.83\left(\frac{D_C - D_p}{D_C}\right)u_g^{0.21}$
Muroyama et al. [14]	2001	Internals	$\mathrm{Nu}_{D_p} = 0.133\mathrm{Pr}^{1/3}(E^{1/3}D_p^{4/3}/\nu)^{0.709}$

[1] We make the simplification of $0.18\epsilon^{1/3} = 0.14u_g^{2/9}$ made by Konsetov based on a correlation by Kutateladze [12]

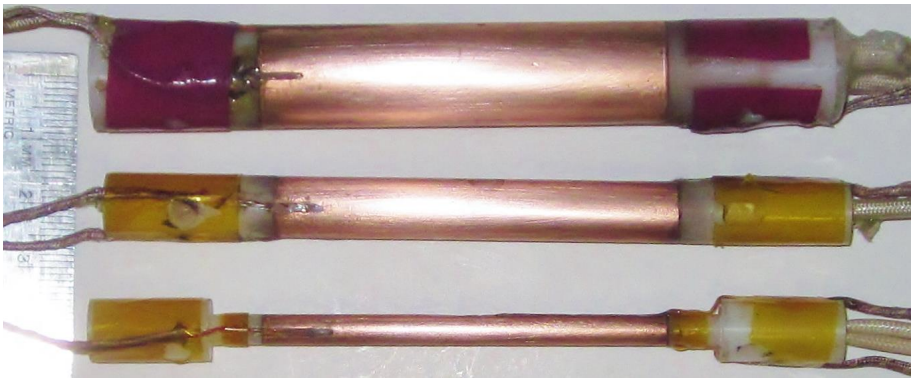

Fig. 1 The three heat transfer coefficient probes

2. METHODS

The heat transfer coefficient outside a coil in a shallow bubble column is measured with three cylindrical heat transfer coefficient probes of different diameters. Gas superficial velocity, probe diameter, liquid height, probe height, and horizontal cylinder position with respect to the sparger holes are varied.

2.1 Heat Transfer Coefficient Probe Design

The heat transfer coefficient probes, shown in Fig. 1, dissipate a known power over a known area and measure the surface and fluid temperatures. Each probe consists of a cartridge heater encased in a copper tube instrumented with several thermocouples. The ends are sealed and insulated with acetal caps ($k_{acetal} = 0.33$ W/m-K [16]). A separate thermocouple measures the bubble column bulk temperature, T_∞. The heat transfer coefficient can then be calculated from measurements, taking into account heat lost through the end caps, using the following equations:

$$\overline{h} = \frac{\dot{Q}_p - 2\dot{Q}_{end}}{A_p(T_{p,ave} - T_\infty)}, \tag{2}$$

where the power dissipated is:

$$\dot{Q}_p = \frac{V^2}{R_e} \tag{3}$$

and where the heat lost at each end (around 1%) is approximately:

$$\dot{Q}_{end} \approx \sqrt{\overline{h} P_p k_{acetal} A_{c,p}}\,(T_{end,ave} - T_\infty). \tag{4}$$

$T_{end,ave}$ is the average reading of the two thermocouples closest to the end caps. The infinitely-long fin approximation of Equation 4 can be applied to the end caps because each is much longer than its extinction length, as shown by Equation 5:

$$(mL)_{end} = \sqrt{\frac{\overline{h} P_p}{k_{acetal} A_{c,p}}}\, L_{end} \approx 18 \text{ to } 120 \gg 1. \tag{5}$$

Cylinders are used to represent coils of large turn radius compared to the outer diameter of the tube. The cylinders have a 62.2 mm-long heated copper test section with 25.4 mm-long press-fit acetal end caps. The probes are 4.76 mm, 9.53 mm, and 15.88 mm (3/16”, 3/8”, and 5/8”) in diameter. As shown in Fig. 2, silicone

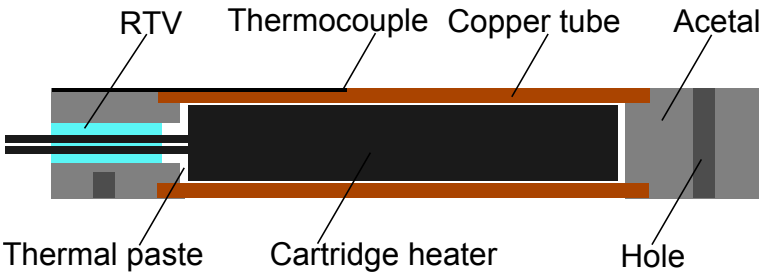

Fig. 2 Schematic diagram showing the heat transfer coefficient probe construction

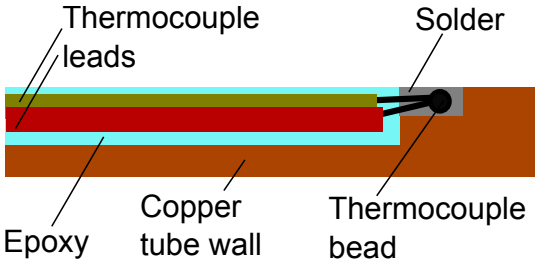

Fig. 3 Schematic diagram showing the embedding of thermocouples in the copper tube wall of the heat transfer coefficient probe

thermal paste is used to fill any air gaps inside the probes.

Thermocouples are distributed in a spiral, covering the probe evenly in both axial and radial directions. Three, four, and five thermocouples are used on the small, medium, and large probes, respectively, with the aim of balancing the accuracy of the average temperature measurement with the risk of altering the heat transfer by adding resistance and surface roughness. The thermal boundary layer thickness outside the internals in a bubble column is comparable in thickness to a human hair ($\sim$100 μm based on 6000 W/m^{2}K in water), so any protrusion away from the surface could alter the heat transfer coefficient at the thermocouple location. The use of even a thin tape to attach the thermocouple would introduce a conduction resistance of similar magnitude as the convection resistance to the column fluid, significantly raising the surface temperature measurement.

To avoid changing the roughness or adding resistance, the thermocouples were embedded in solder-filled troughs cut into the copper tube. Because solder does not adhere well to thermocouple metals, the thermocouple was encased in solder in a solid (but ductile) state. A hand-held butane torch was used to fill the thermocouple bead pocket with solder, leaving a slight hill on top. A trench was cut into the solidified solder bead and the thermocouple bead was placed in the bottom of the trench. An awl was used to press the solder closed around the thermocouple bead. Pressure above 100 bar (in this case, body weight on a $\sim$2 mm square) was applied to form the ductile solder around the thermocouple bead, expelling air and reducing the contact resistance as much as possible. A fine file was used to smooth the cylindrical probe surface. The thermocouple leads were glued into the trench with epoxy. After curing, the epoxy was also filed down and the entire probe was sanded and coarsely polished to discourage outgassing on the probe.

The heat transfer coefficient probes are designed to be accurate within 10-15%. Individual thermocouples have an error of 1.1°C, and there is additional error related to calculating the average temperature of the probe surface with only a few measurements. Considering both of these sources of error, the 4.76 mm, 9.53 mm, and 15.88 mm probes have 95% confidence intervals of 13.7%, 12.4%, and 11.6%, respectively, in the heat transfer coefficient measurement [20]. A significant fraction of the error was due to the necessity of keeping a low temperature difference between the probe and the water to reduce outgassing on the probe.

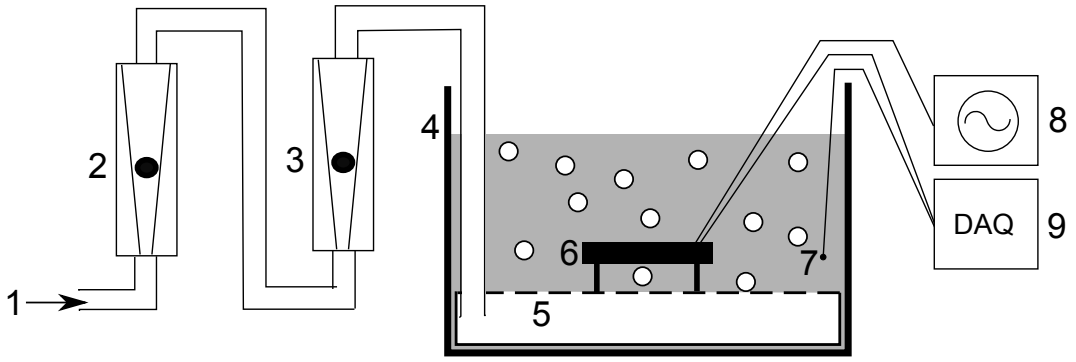

Fig. 4 Experimental apparatus: 1. Pressurized dry air inlet; 2. Rotameter (4-40 cfm); 3. Rotameter (0.4-4 cfm); 4. Tank; 5. Orifice plate sparger; 6. Heat transfer coefficient probe; 7. Thermocouple; 8. Variable autotransformer; 9. Data acquisition unit

2.2 Fixture Design

Figure 4 shows the experimental setup, which allows the gas velocity, liquid depth, sparger design, and cylinder diameter, height, and horizontal position relative to the sparger orifices to be easily varied. The bubble column is contained by a rectangular polycarbonate (PC) tank, 157 mm wide by 284 mm long, which can be filled to a maximum depth of 110 mm above the sparger plate. The tank cross-sectional area can be considered to be large based on observations about tall bubble columns: at a hydraulic diameter of 202 mm, the gas holdup is independent of column diameter [9] and the heat transfer coefficient is within 10% of the large-diameter value [7].

The modular gas sparger uses a replaceable PC sparger plate which is held in place with wing nuts and sealed with a neoprene o-ring. Two sets of holes in the sparger plate are used to attach the probe at the desired height and either above or away from the middle two orifices. All results reported here use a plate with sixteen orifices, each 3 mm in diameter.

2.3 Experimental Protocol

First, tap water is degassed by boiling and cooling. The probe is polished to remove oxidation and installed in the desired position. The column is filled with degassed water to the desired depth during air sparging at 1 cm/s. A wide ruler is positioned a few millimeters from the front wall of the tank to damp the liquid depth fluctuations in the vicinity of the depth measurement without causing significant capillary rise. The heater and DAQ are turned on, and the heater voltage is measured. Ice and/or hot degassed water are added until the column reaches 20°C. The system is allowed a few minutes to reach a quasi-steady state in which there is a constant temperature difference between the probe surface and column liquid.

To make each measurement, the air flow rate is set and the system is given about one minute to return to a quasi-steady state. The air bubbles that accumulate on the warm probe due to the outgassing of air from the water [1] (which, despite initial degassing efforts, tends to reabsorb air during bubbling) are brushed off with a curved pipe cleaner. Because of this bubble-removal procedure, these measurements apply to heat transfer coefficients in cooling, which is the direction of heat transfer in dehumidification and many chemical processing applications, including Fischer-Tropsch synthesis [4]. Finally, approximately sixty measurements of each temperature are taken with the DAQ at half-second intervals. The average temperature of each thermocouple is recorded for use in computing the heat transfer coefficient. This procedure is repeated for a number of air flow rates for each column-probe configuration.

Throughout the experiment, bulk liquid temperature is maintained as close as possible to 20°C. The standard

deviation in bulk temperature was 0.6°C, indicating that the relevant liquid properties (notably the viscosity, density, and thermal conductivity) can be considered constant across all measurements.

2.4 Probe Validation

To test the accuracy of the heat transfer coefficient probes, they were used to measure the well-studied heat transfer coefficient of natural convection on a horizontal cylinder. Each cylinder was immersed in a tank of degassed water, 8.9 cm deep, at a height of 3.7 cm. Measurements are compared in Fig. 5 to a correlation by Churchill and Chu [2] for natural convection on a horizontal cylinder in a large volume. Heat losses from the insulated probe ends were accounted for using Equation 4. In this test, the 4.76 mm, 9.53 mm, and 15.88 mm probes have 95% confidence intervals of 5.8%, 5.3%, and 5.0%, respectively [20]. The probes have a higher accuracy in the natural convection test than in the heat transfer coefficient measurement because this test was conducted with a higher temperature difference (~ 15°C) between the probe and liquid. As shown in Fig. 5, all three probes measured heat transfer coefficients with a nearly-constant average deviation of 7.0% and a maximum deviation of 8.1% from the expected value, both of which are within the accuracy of the correlation itself.

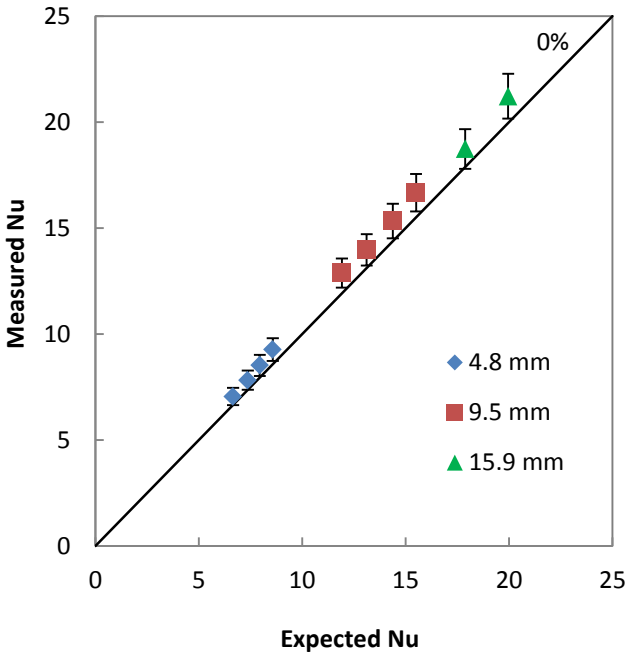

Fig. 5 Probe validation in horizontal natural convection

3. RESULTS AND DISCUSSION

Superficial velocity, probe diameter, liquid depth, probe height[2], and horizontal probe position with respect to the sparger holes[3] were varied to determine the effects of geometry and air velocity on the heat transfer coefficient. Apart from the cylinder diameter, all variables were observed to have a significant effect on the heat transfer coefficient.

[2]Probe height is measured from the top of the sparger plate to the bottom of the probe.
[3]Bubble-on-coil impact is controlled by changing the horizontal position of the cylinder with respect to the sparger orifices so that the probe is positioned over the holes in cases of impact.

Figure 6 compares heat transfer coefficient measurements made using the 4.76 mm-diameter probe at a height of 2 cm with impact to the correlations in Table 1. The shape of the velocity dependence is generally consistent with all three correlations. The data demonstrate good agreement with the correlation of Saxena and Patel [17]. The correlation of Korte [11] for tube bundles, taken at an area fraction of unity to approximate the case of a single tube, also shows good agreement with the data. The correlations of Deckwer [3], Konsetov [10], and Muroyama et al. [14] significantly underpredict the present results.

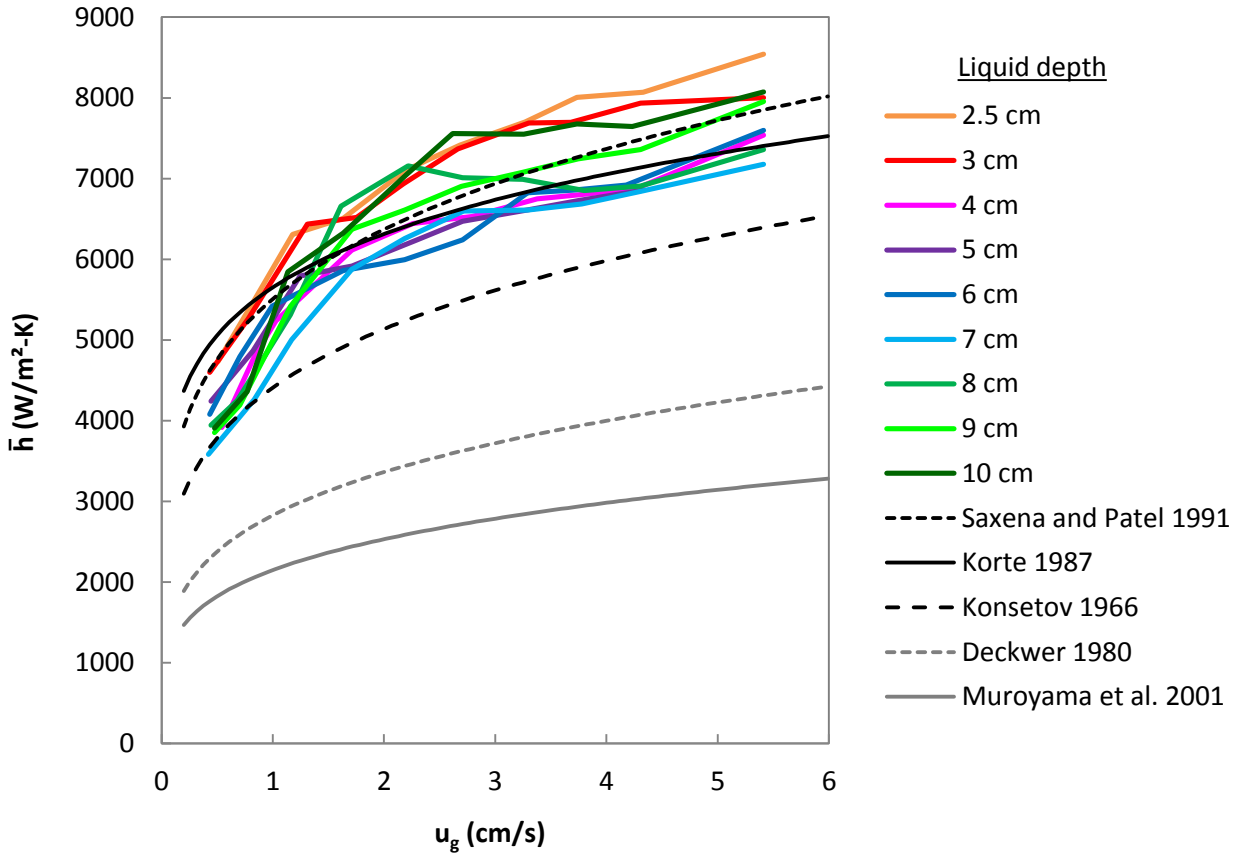

Fig. 6 Experimental data for heat transfer coefficient as a function of superficial velocity over a range of liquid depths are presented along with correlations from literature (Table 1). These results were gathered with the 4.76 mm probe at a height of 2 cm with bubble-on-coil impact.

Figure 6 also shows that the effect of liquid depth on the heat transfer coefficient is not very pronounced.

In Fig. 7, which includes data from the 9.53 mm probe spanning a variety of liquid depths and probe heights, it is clear that neither the correlation of Saxena and Patel [17] nor that of Korte [11] captures all effects of geometry. In particular, the experimental data at low (<2 cm) probe height is much lower than predicted by these correlations. The Korte correlation also seems to overpredict the effect of probe diameter on heat transfer coefficient. Clearly, many variables affect the heat transfer coefficient in a shallow bubble column. These effects are analyzed in the coming sections.

3.1 Cylinder Diameter

The effect of cylinder diameter was investigated because of disagreement among correlations in the literature. Figure 8 shows the relative insensitivity of the heat transfer coefficient to cylinder diameter for probes between 4.76 and 15.88 mm in diameter. It is clear from Fig. 8 that the effect is not as pronounced as in Konsetov's

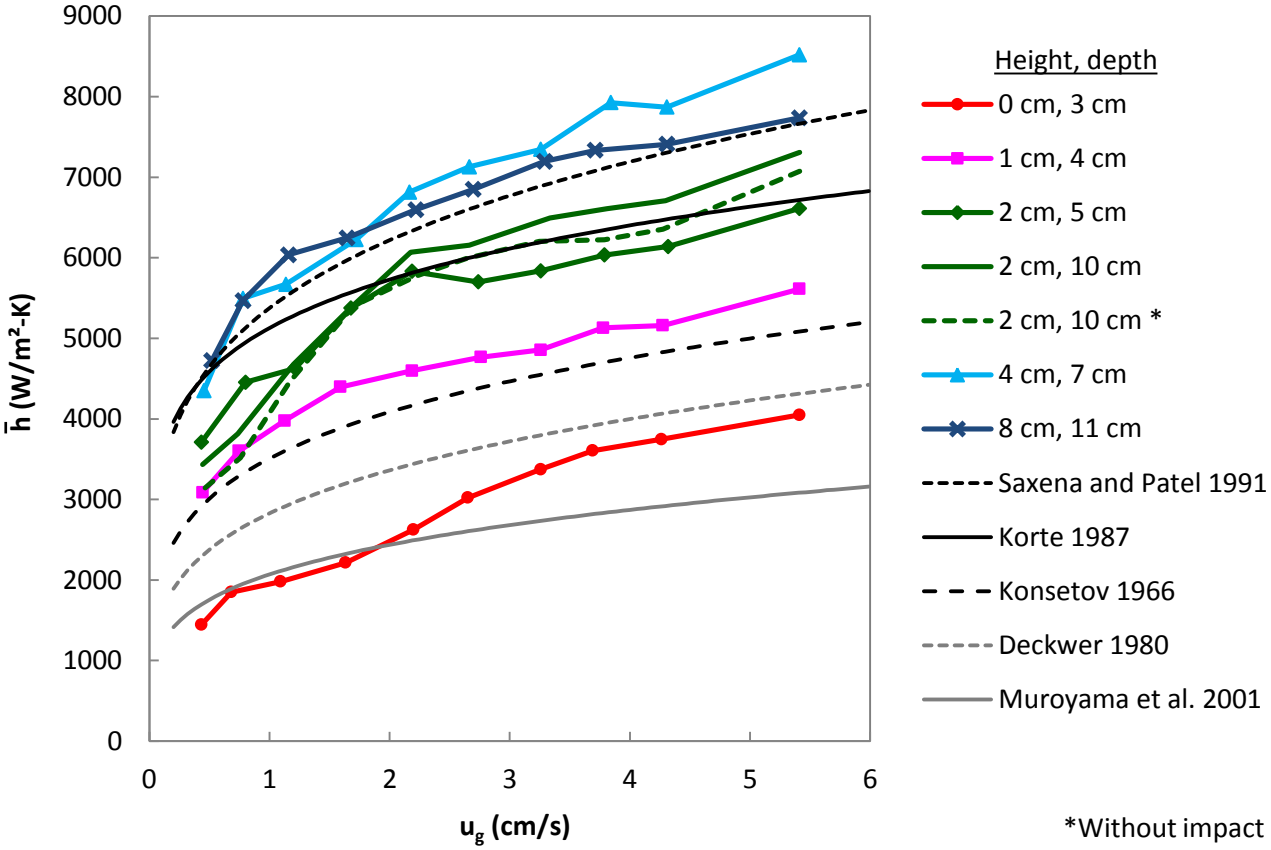

Fig. 7 Experimental data for the heat transfer coefficient on the 9.53 mm probe as a function of superficial velocity over a range of probe heights and liquid depths are presented along with several correlations. All results are with bubble-on-coil impact except where noted.

model, in which the heat transfer coefficient is proportional to the -1/3 power of probe diameter. This result hints at the difference in length scale between the probe and the relevant fluid structure in the multiphase flow. It is clear that the length scale of the relevant fluid structure (whose identity is a subject of disagreement) is much smaller than the diameter of these probes.

It is immediately clear that the effects of probe diameter are insignificant compared to the effects of the other geometric parameters causing the spread in Fig. 7. The 11-14% error in the measurements of the probes, discussed in Section 2.1, may account for the spread in Fig. 8. For cylinders placed at 2 cm height in 10 cm-deep water, Fig. 8 also shows that bubble-on-coil impact does not significantly affect the heat transfer coefficient.

3.2 Cylinder Height

In shallow bubble columns, the heat transfer coefficient depends on the height of the cylinder. Cylinder height is defined as the distance between the sparger plate and the bottom of the cylinder. The effect of cylinder height on heat transfer coefficient is shown in Fig. 9. In Fig. 9, the distance from the top of the fluid to the top of the cylinder is held constant. The heat transfer coefficient increases monotonically with height until reaching a maximum at 4 cm in both regions. Similar but slightly lower heat transfer coefficients are measured for 6 and 8 cm heights. The drop in heat transfer coefficient as the probe height is reduced from 4 to 0 cm is unsurprising because the wall acts as a momentum sink, decreasing the specific kinetic energy in its vicinity. The peak in

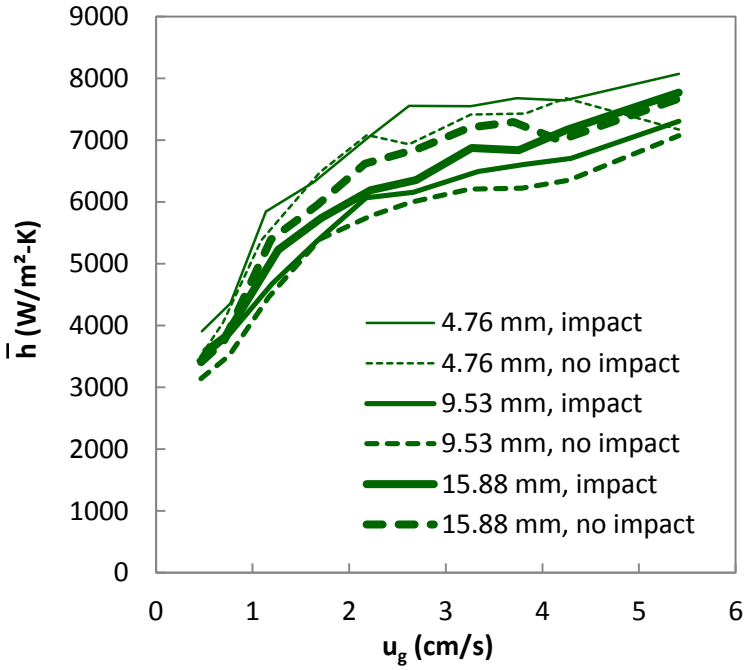

Fig. 8 Heat transfer coefficient at 2 cm probe height and 10 cm liquid depth for all three cylinder diameters, with and without impact

heat transfer coefficient around a height of 4 cm is most likely due to the height-dependent bubble dynamics near the sparger.

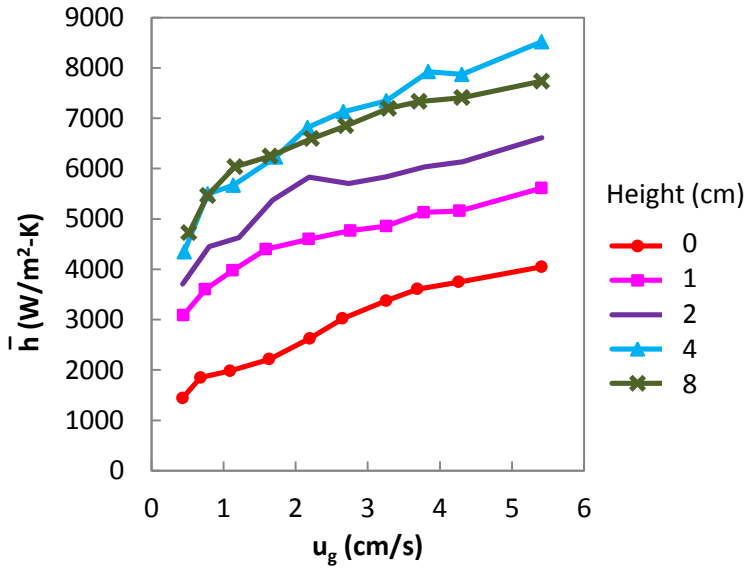

Fig. 9 Heat transfer coefficients with impact on the 9.53 mm probe at a variety of heights. In each measurement, the fluid level is maintained 2 cm over the top of the probe.

3.3 Design Recommendations

The results presented here inform the effective and economical design of bubble column dehumidifiers. The cooling coil of a bubble column dehumidifier should be placed at a height of around 4 cm where the heat transfer coefficient is highest, which is also tall enough for effective gas-liquid contact [23]. Given that the diameter of the coil has no significant effect on the outer heat transfer coefficient, the diameter needs to be optimized based on the internal heat transfer coefficient [13] and friction factor only.

4. CONCLUSIONS

The heat transfer coefficient on a cylinder in a bubble column is measured with horizontal cylindrical probes to elucidate the effects of geometric parameters specific to shallow bubble columns. Sufficiently far from the sparger, there is good agreement with the correlations of Korte [11] and Saxena and Patel [17]. Near the sparger, heat transfer coefficient is shown to increase with cylinder height until reaching a maximum at 4 cm. Cylinder diameter and liquid depth have little effect on heat transfer. These results inform the design of effective and economical bubble column dehumidifiers.

ACKNOWLEDGMENTS

We would like to acknowledge support from the King Fahd University of Petroleum and Minerals through the Center for Clean Water and Clean Energy at MIT and KFUPM (Project #R4-CW-08). EWT would also like to gratefully acknowledge support from the Flowers Family Fellowship and the Pappalardo Fellowship and thank Immanuel David Madukauwa-David for taking the preliminary measurements which guided the direction of this experiment. This material is based upon work supported by the National Science Foundation Graduate Research Fellowship Program under Grant No. 1122374.

NOMENCLATURE

Roman					
A_f	Free area fraction [10]	[-]	T	Temperature	[K]
D	Diameter	[m]	u_g	Superficial velocity $= \dot{V}/A_C$	[m/s]
E	Specific power dissipation [14]	[W/kg]	V	Voltage	[V]
Fr	Froude number = $u_g^2/(gD)$	[-]	$\dot{V}$	Gas volume flow rate	[m^3/s]
g	Gravitational acceleration	[m/s^2]	Greek		
$\overline{h}$	Average heat transfer coefficient	[W/m^2-K]	ϵ	Gas volume fraction	[-]
k	Thermal conductivity of liquid	[W/m-K]	μ	Dynamic viscosity of liquid	[Pa-s]
L	Length	[m]	ν	Kinematic viscosity of liquid	[m^2/s]
m	Fin parameter	[m^{-1}]			
Nu	Nusselt number	[-]	Subscripts		
P	Wetted perimeter	[m]	∞	Liquid bulk	
Pr	Prandtl number	[-]	ave	Average	
$\dot{Q}$	Heat transfer rate	[W]	C	Column	
R_e	Electrical resistance	[Ω]	c	Cross-sectional	
Re	Reynolds number	[-]	end	Probe end cap	
St	Stanton number	[-]	p	Probe	

REFERENCES

[1] Battino, R. and Clever, H. L., "The solubility of gases in liquids," *Chemical Reviews*, 66(4), pp. 395–463, (1966).

[2] Churchill, S. W. and Chu, H. H., "Correlating equations for laminar and turbulent free convection from a horizontal cylinder," *International Journal of Heat and Mass Transfer*, 18(9), pp. 1049 – 1053, (1975).

[3] Deckwer, W.-D., "On the mechanism of heat transfer in bubble column reactors," *Chemical Engineering Science*, 35(6), pp. 1341 – 1346, (1980).

[4] Deckwer, W.-D., Louisi, Y., Zaidi, A., and Ralek, M., "Hydrodynamic properties of the fischer-tropsch slurry process," *Industrial & Engineering Chemistry Process Design and Development*, 19(4), pp. 699–708, (1980).

[5] Hikita, H., Asai, S., Tanigawa, K., Segawa, K., and Kitao, M., "Gas hold-up in bubble columns," *The Chemical Engineering Journal*, 20(1), pp. 59 – 67, (1980).

[6] Hulet, C., Clement, P., Tochon, P., Schweich, D., Dromard, N., and Anfray, J., "Literature review on heat transfer in two- and three-phase bubble columns," *International Journal of Chemical Reactor Engineering*, 7(1), pp. –, (2009).

[7] Jhawar, A. K. and Prakash, A., "Heat transfer in a slurry bubble column reactor: A critical overview," *Industrial & Engineering Chemistry Research*, 51(4), pp. 1464–1473, (2012).

[8] Kagumba, M. O. O., Heat transfer and bubble dynamics in slurry bubble columns with internals for Fischer-Tropsch synthesis of clean alternative fuels and chemicals, PhD thesis, Missouri University of Science and Technology, (2013).

[9] Kantarci, N., Borak, F., and Ulgen, K. O., "Review: Bubble column reactors," *Process Biochemistry*, 40(7), pp. 2263–2283, (2005).

[10] Konsetov, V., "Heat transfer during bubbling of gas through liquid," *International Journal of Heat and Mass Transfer*, 9(10), pp. 1103 – 1108, (1966).

[11] Korte, H., Heat transfer in bubble columns with and without internals, PhD thesis, University of Dortmund, (1987).

[12] Kutateladze, S. S. and Styrikovich, M. A., *Hydraulics of gas-liquid systems*, Gosenergoizdat, (1959).

[13] Mori, Y. and Nakayama, W., "Study on forced convective heat transfer in curved pipes: (1st report, laminar region)," *International Journal of Heat and Mass Transfer*, 8(1), pp. 67 – 82, (1965).

[14] Muroyama, K., Okumichi, S., Goto, Y., Yamamoto, Y., and Saito, S., "Heat transfer from immersed vertical cylinders in gas-liquid and gas-liquid-solid fluidized beds," *Chemical Engineering & Technology*, 24(8), pp. 835–842, (2001).

[15] Narayan, G. P., Sharqawy, M. H., Lam, S., Das, S. K., and Lienhard V, J. H., "Bubble columns for condensation at high concentrations of noncondensable gas: Heat-transfer model and experiments," *AIChE Journal*, 59(5), pp. 1780–1790, (2013).

[16] Samyn, P. and Baets, P. D., "Friction and wear of acetal: A matter of scale," *Wear*, 259(16), pp. 697 – 702, (2005).

[17] Saxena, S. and Patel, B., "Heat transfer investigations in a bubble column with immersed probes of different diameters," *International Communications in Heat and Mass Transfer*, 18(4), pp. 467 – 478, (1991).

[18] Saxena, S. and Rao, N., "Heat transfer and gas holdup in a two-phase bubble column: Air-water system – review and new data," *Experimental Thermal and Fluid Science*, 4(2), pp. 139 – 151, (1991).

[19] Schluter, S., Steiff, A., and Weinspach, P.-M., "Heat transfer in two- and three-phase bubble column reactors with internals," *Chemical Engineering and Processing: Process Intensification*, 34(3), pp. 157 – 172, (1995).

[20] Tow, E. W., (2014). "Heat and mass transfer in bubble column dehumidifiers for HDH desalination," . Master's thesis, Massachusetts Institute of Technology.

[21] Tow, E. W. and Lienhard V, J. H., "Analytical modeling of a bubble column dehumidifier," *Proceedings of the ASME Summer Heat Transfer Conference, Minneapolis, MN, July 14-19, 2013*, (2013), paper #HT2013-17763.

[22] Tow, E. W. and Lienhard V, J. H., "Heat flux and effectiveness in bubble column dehumidifiers for HDH desalination," *Proceedings of the International Desalination Association World Congress on Desalination and Water Reuse, Tianjin, China, Oct 20-25*, (2013).

[23] Tow, E. W. and Lienhard V, J. H., "Experiments and modeling of bubble column dehumidifier performance," *International Journal of Thermal Sciences*, 80(0), pp. 65–75, (2014).